Electronic Supplementary Information

Stabilization of hydrogen peroxide by hydrogen bonding in the crystal structure of 2-aminobenzimidazole perhydrate

Andrei V. Churakov,[a] Dmitry A. Grishanov,[a,b] Alexander G. Medvedev,[a] Alexey A. Mikhaylov,[a] Mikhail V. Vener,[a,c] Mger A. Navasardyan,[a] Tatiana A. Tripol'skaya,[a] Ovadia Lev[b] and Petr V. Prikhodchenko*[a]*

[a]Kurnakov Institute of General and Inorganic Chemistry, Russian Academy of Sciences, Leninskii prosp. 31, Moscow 119991, Russia

[b]The Casali Center and the Institute of Chemistry and The Harvey M. Krueger Family Center for Nanoscience and Nanotechnology, The Hebrew University of Jerusalem, Edmond J. Safra Campus, Jerusalem 91904, Israel

[c]Department of Quantum Chemistry, D. Mendeleev University of Chemical Technology, Miusskaya Square 9, Moscow 125047, Russia

Contents

1. Experimental details S3

1.1. Elemental analysis S3

1.2. IR spectra S3

2. Computational details S3

2.1. Solid-State DFT Followed by Bader Analysis of the Periodic Electronic Density S3

2.2. Evaluation of H-bond enthalpies/energies S4

Table S1 S4

Table S2 S5

Table S3 S5

Table S4 S5

References S6

1. Experimental details

1.1. Elemental analysis

Peroxide content was estimated by permanganometry. Carbon, hydrogen and nitrogen content was determined using the Perkin-Elmer 2400 series II Analyzer (CHN).

Anal. Calc. for $C_{14}H_{16}N_6O_2$ (**I**): OO (peroxide), 11.58; N, 27.98; C, 55.99; H, 5.37. Found: OO (peroxide), 11.42; N, 27.75; C, 55.89; H, 5.35.

1.3. IR spectra

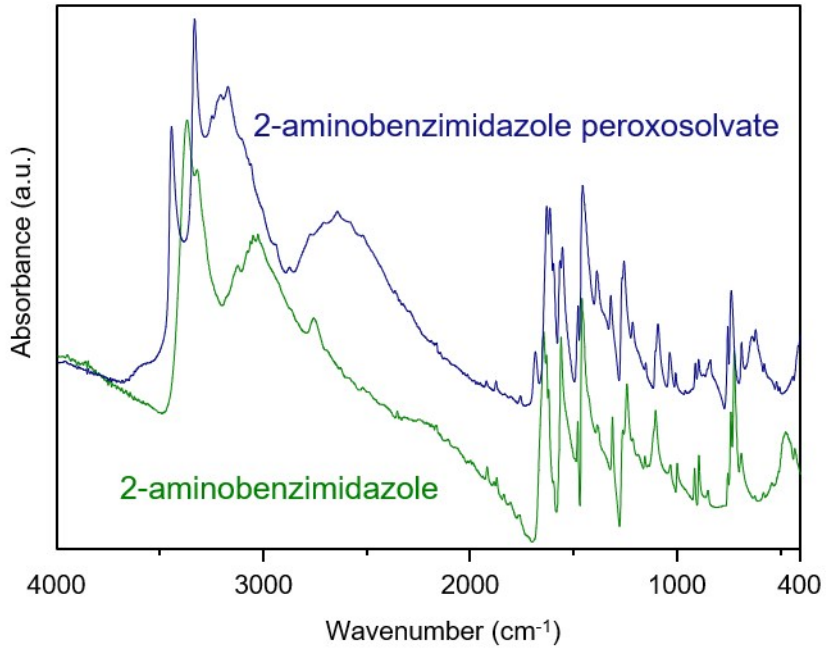

Fig. S1. FTIR spectra of 2-aminobenzimidazole peroxosolvate (**I**) and 2-aminobenzimidazole crystals.

2. Computational details

2.1. Periodic (Solid-State) DFT Followed by Bader Analysis of the Crystalline Electronic Density.

The space groups and unit cell parameters of the considered two-component crystals (**I**, **III**[1] and L-serine peroxosolvate[2]) obtained in the single-crystal X-ray studies are fixed and structural

relaxations are limited to the positional parameters of atoms. The atomic positions from experiment are used as the starting point in the solid-state DFT computations. Density functional theory computations with periodic boundary conditions (solid-state DFT) were performed in the Crystal09 software package[3,4] using PBE functional in the localized basis set 6-31+G** for N,O atoms and 6-31G** for C,H atoms. The PBE/6-31+G** approximation provides reliable and consistent results in studying the intermolecular interactions in crystals.[5] The mixing coefficient of Hartree-Fock/Kohn-Sham matrices is set to 25%. Tolerance on energy controlling the self-consistent field convergence for geometry optimizations and frequencies computations is set to 10^{-10} hartree. The shrinking factor of the reciprocal space net is set to 4. All the optimized structures are found to correspond to the minimum point on the potential energy surface.

2.2. Evaluation of H-bond energies

The optimized structures were used in PBE/6-31+G** computations of the periodic electronic wave-functions by CRYSTAL98.[6] The quantum theory of atoms in molecules and crystals (Bader) analysis of the crystalline electron density[7] is performed with TOPOND.[8] The calculation methodology is presented elsewhere.[9,10] The energy of the considered hydrogen bond, energy E_{HB}, is evaluated according to ref. 11 as:

$$E_{HB}\ [\text{kJ mol}^{-1}] = 1124 \cdot G_b\ [\text{atomic units}], \qquad \text{(S1)}$$

where G_b is the positively-defined local electronic kinetic energy density at the H···O bond critical point. Eq. (1) yields reasonable E_{HB} values for molecular crystals with intermolecular H-bonds.[12]

Table S1. Optimized parameters of the selected geometrical parameters in **I** at PBE/6-31+G** level vs experimental data.

Fragment	Experimental	PBE/6-31+G**
H_2O_2 molecule		
d(O-O), Å	1.4747(14)	1.475
d(O-H), Å	0.923(16)	1.038
∠(O-O-H), °	97.7(10)	98.684
∠(H-O-O-H),°	110(2)	111.969
$C_7H_7N_3$ molecule		
d(C_1-N_1), Å	1.347(1)	1.352
d(N_1-H), Å	0.876(16)	1.021
	0.888(16)	1.027
d(N_3-H), Å	0.891(15)	1.037
∠(N-C-N-H),°	14	14.537

Table S2. Computed values of the electron density, ρ_b, and the local electronic kinetic energy density, G_b, at the D…A (D, A=O, N) bond critical point and the H-bond energy E_{HB} evaluated using Eq. S1 in **III**.

H-bonded fragment[a]	d(D…A), Å		ρ_b (a.u.)	G_b (a.u.)	E_{HB}, (kJ mol^{-1})
	Exp[13]	Calcd			
O(2)-H···N(5C)	2.721(1)	2.691	0.0596	0.0351	**39.5**
O(1)-H···N(6)	2.706(1)	2.684	0.0614	0.0359	**40.4**
N(1A)-H···O(1)	2.947(1)	2.925	0.0293	0.0206	**23.2**
N(3B)-H···O(1)	3.004(1)	2.983	0.0199	0.0146	**16.5**
N(2E)-H···O(2)	3.035(1)	3.059	0.0140	0.0106	**12.0**
N(5C)-H···O(2)	3.187(1)	3.186	0.0093	0.0072	**8.1**

[a] See Fig. **3b**.

Table S3. Computed values of the electron density, ρ_b, and the local electronic kinetic energy density, G_b, at the D…A (D, A=O, N) bond critical point and the H-bond energy E_{HB} evaluated using Eq. S1 in **L-serine peroxosolvate**.

H-bonded fragment[a]	d(D…A), Å		ρ_b (a.u.)	G_b (a.u.)	E_{HB}, (kJ mol^{-1})
	Exp[14]	Calcd			
Op-H···O-H(serine)	2.692(2)	2.627	0.0527	0.0394	**44.4**
Op-H···O-C-O$^-$(serine)	2.716(2)	2.692	0.0414	0.0315	**35.5**
Op···H-N (serine)	2.833(2)	2.777	0.0287	0.0219	**24.7**
Op···H-N (serine)	2.876(2)	2.911	0.0092	0.0077	**8.7**

[a] Op denotes O atom of hydrogen peroxide molecule.

Table S4. Computed values of the electron density, ρ_b, and the local electronic kinetic energy density, G_b, at the O…O bond critical point and the H-bond energy E_{HB} evaluated using Eq. S1 in **H_2O_2**.

H-bonded fragment	d(D…A), Å		ρ_b (a.u.)	G_b (a.u.)	E_{HB}, (kJ mol^{-1})
	Exp[15]	Calcd			
O-H···O	2.758(6)	2.689	0.0479	0.0333	**37.5**

References

1 I. Y. Chernyshov, M. V. Vener, P. V. Prikhodchenko, A. G. Medvedev, O. Lev and A. V. Churakov, *Cryst. Growth Des.*, 2017, **17**, 214–220.

2 M. V Vener, A. G. Medvedev, A. V Churakov, P. V Prikhodchenko, T. A. Tripol'skaya and O. Lev, *J. Phys. Chem. A*, 2011, **115**, 13657–136663.

3 R. Dovesi, R. Orlando, B. Civalleri, C. Roetti, V. R. Saunders and C. M. Zicovich-Wilson, *Zeitschrift für Krist. - Cryst. Mater.*, 2005, **220**, 571–573.

4 R. Dovesi, V. R. Saunders, C. Roetti, R. Orlando, C. M. Zicovich-Wilson, F. Pascale, B. Civalleri, K. Doll, N. M. Harrison, I. J. Bush, P. D. D'Arco and M. Llunell, *CRYSTAL09 User's Manual*, University of Torino, Torino, 2009.

5 A. G. Medvedev, A. V.Shishkina, P. V. Prikhodchenko, O. Lev and M. V. Vener, *RSC Adv.*, 2015, **5**, 29601–29608.

6 V. R. Saunders, R. Dovesi, C. Roetti, M. Causa, N. M. Harrison, R. Orlando and C. M. Zicovich-Wilson, *Univ. Torino, Torino*, 1998.

7 V. G. Tsirelson, in *The Quantum Theory of Atoms in Molecules*, Wiley-VCH Verlag GmbH & Co. KGaA, Weinheim, Germany, 2007, pp. 257–283.

8 C. Gatti, *CNR-CSRSRC, Milano*, 1999.

9 A. V. Churakov, D. A. Grishanov, A. G. Medvedev, A. A. Mikhaylov, T. A. Tripol'skaya, M. V. Vener, M. A. Navasardyan, O. Lev and P. V. Prikhodchenko, *CrystEngComm*, 2019, **21**, 4961–4968.

10 A. G. Medvedev, A. A. Mikhaylov, I. Y. Chernyshov, M. V. Vener, O. Lev and P. V. Prikhodchenko, *Int. J. Quantum Chem.*, 2019, **119**, e25920.

11 I. Mata, I. Alkorta, E. Espinosa and E. Molins, *Chem. Phys. Lett.*, 2011, **507**, 185–189.

12 S. A. Katsyuba, M. V. Vener, E. E. Zvereva and J. G. Brandenburg, *Chem. Phys. Lett.*, 2017, **672**, 124–127.

13 I. Yu. Chernyshov, M. V. Vener, P. V. Prikhodchenko, A. G. Medvedev, O. Lev and A. V. Churakov, *Cryst. Growth Des.*, 2017, **17**, 214–220.

14 A. V Churakov, P. V Prikhodchenko, J. A. K. Howard and O. Lev, *Chem. Commun.*, 2009, **28**, 4224–4226.

15 J. M. Savariault and M. S. Lehmann, *J. Am. Chem. Soc.*, 1980, **102** (4), 1298-1303.